2

Exact Nonlinear Dynamics in Spinor Bose-Einstein Condensates

Jun'ichi Ieda[1] and Miki Wadati[2]
[1]*Institute for Materials Research, Tohoku University,*
[2]*Department of Physics, Tokyo University of Science*
Japan

1. Introduction

Bose–Einstein Condensation (BEC) of atomic gases has attracted a renewed theoretical and experimental interest in quantum many-body systems at extremely low temperatures (Pethick & Smith; 2002). This excitement stems from two favorable features: (1) by applying magnetic fields and lasers, most of the system parameters, such as the shape, dimensionality, internal states of the condensates, and even the strength of the interatomic interactions, are controllable; (2) due to the diluteness, the mean-field theory explains experiments quite well. In particular, the Gross–Pitaevskii (GP) equation demonstrates its validity as a basic equation for the condensate dynamics. The GP equation is the counterpart of the nonlinear Schrödinger (NLS) equation in nonlinear optics. Thus, a study based on nonlinear analysis is possible and important.

In nonlinear physics, a soliton is remarkable object not only for the fact that exact solutions can be obtained but also for its usefulness as a communications tool due to its robustness. In general, solitons are formed under the balance between nonlinearity and dispersion. For atomic condensates, the former is attributed to the interatomic interactions, while the latter comes from the kinetic energy. Either dark or bright solitons are allowable depending on the positive or negative sign of the interatomic coupling constants g, respectively, and indeed have been observed in a quasione-dimensional (q1D) optically constructed waveguide (Strecker et al.; 2002) (Khaykovich et al.; 2002). Such matter-wave solitons are expected in atom optics for applications in atom laser, atom interferometry, and coherent atom transport (Meystre; 2002). In this chapter, we extend the analysis of the matter-wave solitons to a multicomponent case by considering the so-called spinor condensate (Stenger et al.; 1998) whose spin degrees of freedom are liberated under optical traps. Based on theoretical and experimental results, we introduce a new integrable model which describes the dynamical properties of the matter-wave soliton of spinor condensates (Ieda et al.; 2004a). We employ the inverse scattering method to solve this model exactly. As a result, we predict the occurrence of undiscovered physical phenomena such as macroscopic spin precession and spin switching.

The chapter is organized as follows. In Sec. 2, the mean field theory of condensate is briefly reviewed. Section 3 introduces an effective interatomic coupling in a q1D condensate. Using these results, we consider a spinor condensate in q1D regime in Sec. 4. Then, in Sec. 5, we

Source: Nonlinear Dynamics, Book edited by: Todd Evans,
ISBN 978-953-7619-61-9, pp. 366, January 2010, INTECH, Croatia, downloaded from SCIYO.COM

show an integrable condition of the coupled nonlinear equations for spinor condensates in which the exact soliton solutions are derived. In Sec. 6 and 7, we analyze the spin properties of one-soliton and two-soliton, respectively. Finally we summarize our findings and remark some current progresses on this topic in Sec. 8.

2. Mean field theory

The dynamics of BEC wave function can be described by an effective mean-field equation known as the Gross-Pitaevskii (GP) equation. This is a classical nonlinear equation that takes into account the effects of interatomic interactions through an effective mean field.
In this section, we derive the GP equation for a single component condensate and discuss the theoretical background of it for later extension to a low dimensional case and a spinor case.

2.1 Hamiltonian

In order to derive the mean-field equation for atomic BECs, we start with the second quantized Hamiltonian. The Hamiltonian for the system of N interacting bosons with the mass m in a trap potential $U_{\text{trap}}(\mathbf{r})$ can be written as

$$\hat{H} = \hat{H}_0 + \hat{H}_{\text{int}}, \tag{1}$$

$$\hat{H}_0 = \int \mathrm{d}\mathbf{r}\hat{\Psi}^\dagger(\mathbf{r}) \left[-\frac{\hbar^2}{2m}\nabla^2 + U_{\text{trap}}(\mathbf{r}) \right] \hat{\Psi}(\mathbf{r}), \tag{2}$$

$$\hat{H}_{\text{int}} = \frac{1}{2}\int \mathrm{d}\mathbf{r}\mathrm{d}\mathbf{r}'\hat{\Psi}^\dagger(\mathbf{r})\hat{\Psi}^\dagger(\mathbf{r}')v(\mathbf{r}-\mathbf{r}')\hat{\Psi}(\mathbf{r})\hat{\Psi}(\mathbf{r}'), \tag{3}$$

where $v(\mathbf{r} - \mathbf{r}')$ expresses the two-body interaction and the bosonic field operators satisfy the equal-time commutation relations:

$$[\hat{\Psi}(\mathbf{r}), \hat{\Psi}^\dagger(\mathbf{r}')] = \delta(\mathbf{r}-\mathbf{r}'), \quad [\hat{\Psi}^\dagger(\mathbf{r}), \hat{\Psi}^\dagger(\mathbf{r}')] = [\hat{\Psi}(\mathbf{r}), \hat{\Psi}(\mathbf{r}')] = 0. \tag{4}$$

In most of the experiments, the trap is well approximated by a harmonic oscillator potential,

$$U_{\text{trap}}(\mathbf{r}) = \frac{1}{2}m(\omega_x^2 x^2 + \omega_y^2 y^2 + \omega_z^2 z^2). \tag{5}$$

Condensates are pancake-shape for $\omega_z \gg \omega_{x,y}$ whereas cigar-shape for $\omega_{x,y} \gg \omega_z$. For other choice of trap potentials, say a linear or a 4-th order potential, the thermodynamic properties can be changed (Ieda et al.; 2001). The discussion about non-harmonic potentials will be given in a later section in connection with an implementation of quasi-one dimensional system.
The atom-atom interaction $v(\mathbf{r} - \mathbf{r}')$ in a dilute and ultracold system can be approximated by

$$v(\mathbf{r}-\mathbf{r}') = g\,\delta(\mathbf{r}-\mathbf{r}'), \tag{6}$$

$$g = \frac{4\pi\hbar^2 a}{m}, \tag{7}$$

where a is the s-wave scattering length. The scattering length is the controllable parameter which determines the properties of the low energy scattering between cold atoms. The positive (negative) sign of a corresponds to the effectively repulsive (attractive) interaction.

2.2 Bogoliubov theory

The mean-field theory for *weakly interacting dilute Bose gases* (WIDBG) was proposed in Bogoliubov's 1947 work (Pethick & Smith; 2002). The main idea of his approach consists in separating out the condensate contribution from the bosonic field operator:

$$\hat{\Psi}(\mathbf{r},t) \simeq \sqrt{n_0} + \hat{\phi}(\mathbf{r},t), \tag{8}$$

where $n_0 = N_0/\Omega$ is a uniform condensate density (c-number) with N_0 the number of the condensed atoms, Ω the volume of the system, and the quantum part $\hat{\phi}$ is assumed to be a small perturbation. Taking $\hat{\phi}$ and $\hat{\phi}^\dagger$ terms up to quadratic, Bogoliubov built the "first-oder" theory of uniform Bose gas.

This idea can be extended to non-uniform gases in trap potentials. If we introduce the $\mathbf{r}$ dependence of the condensate part, the field operator is expressed as

$$\hat{\Psi}(\mathbf{r},t) \simeq \Phi(\mathbf{r},t) + \hat{\phi}(\mathbf{r},t). \tag{9}$$

The scalar function $\Phi(\mathbf{r}, t)$ is called the *condensate wave function*, which is normalized to be the number of the condensed atoms,

$$\int \mathrm{d}\mathbf{r}|\Phi(\mathbf{r})|^2 = N_0. \tag{10}$$

In the case of BEC, the number of the condensed atoms becomes macroscopic, i.e.,

$$N - N_0 \ll N_0 < N. \tag{11}$$

In this sense, the "macroscopic" wave function $\Phi(\mathbf{r}, t)$ is related to the first quantized N-body wave function $\Phi_N(\mathbf{r}_1, \ldots, \mathbf{r}_N; t)$ as

$$\Phi_N(\mathbf{r}_1,\ldots,\mathbf{r}_N;t) \simeq \Pi_i \Phi(\mathbf{r}_i,t), \tag{12}$$

which obviously satisfies the symmetry under exchanges of two bosons.

Following the Bogoliubov prescription, we substitute (9) into (1) and retain $\hat{\phi}$ and $\hat{\phi}^\dagger$ terms up to quadratic;

$$\hat{H} \simeq E_\Phi + \hat{H}_1 + \hat{H}_2, \tag{13}$$

$$E_\Phi = \int \mathrm{d}\mathbf{r}\Phi^*(\mathbf{r},t)\left[-\frac{\hbar^2}{2m}\nabla^2 + U_{\mathrm{trap}}(\mathbf{r}) + \frac{g}{2}|\Phi(\mathbf{r},t)|^2\right]\Phi(\mathbf{r},t), \tag{14}$$

$$\hat{H}_1 = \int \mathrm{d}\mathbf{r}\Phi^*(\mathbf{r},t)\left[-\frac{\hbar^2}{2m}\nabla^2 + U_{\mathrm{trap}}(\mathbf{r}) + g|\Phi(\mathbf{r},t)|^2\right]\hat{\phi}(\mathbf{r},t) + \mathrm{h.c.}, \tag{15}$$

$$\hat{H}_2 = \int \mathrm{d}\mathbf{r}\hat{\phi}^\dagger(\mathbf{r},t)\left[-\frac{\hbar^2}{2m}\nabla^2 + U_{\mathrm{trap}}(\mathbf{r}) + 2g|\Phi(\mathbf{r},t)|^2\right]\hat{\phi}(\mathbf{r},t) + \frac{g}{2}\int \mathrm{d}\mathbf{r}\left[\hat{\phi}^\dagger(\mathbf{r},t)\hat{\phi}^\dagger(\mathbf{r},t)\Phi(\mathbf{r},t)^2 + \Phi^*(\mathbf{r},t)^2\hat{\phi}(\mathbf{r},t)\hat{\phi}(\mathbf{r},t)\right]. \tag{16}$$

Equation (14) is called the Gross-Pitaevskii energy functional. The statistical and dynamical properties of the condensate are determined through a variation of E_Φ while the low-lying excitations from the ground state can be analyzed by diagonalizing $\hat{H}_2$. In the ground state, $\hat{H}_1$ part vanishes identically.

2.3 Gross-Pitaevskii equation

Even at the zero temperature, interactions may cause quantum correlation which gives rise to occupation in the excited states. The assumption that the quantum fluctuation part $\hat{\phi}$ (**r**, *t*) gives a small contribution to the condensate is valid for a dilute system. In particular, if we consider a dilute limit:

$$na^3 \ll 1, \tag{17}$$

where na^3 is the gas parameter with n the particle number density, neglecting $\hat{\phi}$ parts provides an appropriate description of the condensate wave function at zero temperature. By a variational principle,

$$\imath\hbar\frac{\partial}{\partial t}\Phi(\mathbf{r},t) = \frac{\delta E_\Phi}{\delta\Phi^*(\mathbf{r},t)}, \tag{18}$$

we obtain the Gross-Pitaevskii (GP) equation:

$$\imath\hbar\frac{\partial}{\partial t}\Phi(\mathbf{r},t) = \left[-\frac{\hbar^2}{2m}\nabla^2 + U_{\mathrm{trap}}(\mathbf{r}) + g|\Phi(\mathbf{r},t)|^2\right]\Phi(\mathbf{r},t). \tag{19}$$

This equation has been derived independently by Gross and Pitaevskii (Pethick & Smith; 2002) to deal with the superfluidity of ^{4}He-II. The GP equation is a classical field equation for a scalar (complex) function Φ but contains $\hbar$ explicitly. In this sense, the description of the condensate in terms of Φ is a manifestation of the macroscopic de Broglie wave, where the corpuscular aspect of matter dose not play a role. Now the modulus and gradient of phase of $\Phi = |\Phi|\exp(\imath\varphi)$ have a clear physical meaning,

$$n(\mathbf{r},t) = |\Phi(\mathbf{r},t)|^2, \qquad \mathbf{v}(\mathbf{r},t) = \frac{\hbar}{m}\nabla\varphi(\mathbf{r},t), \tag{20}$$

where n and **v** denote number density and velocity of the condensate, respectively.

3. Confinement induced resonance

In this section, we derive an effective one-dimensional (1D) Hamiltonian for bosons confined in an elongated trap. The interactions between atoms in the experiments are always three-dimensional (3D) even when the kinetic motion of the atoms in such a tight radial confinement is 1D like. Therefore, the trap-induced corrections to the strength of the atomic interactions should be taken into account properly.

This problem was first solved by Olshanii (Olshanii; 1998) within the pseudopotential approximation, yielding a new type of tuning mechanism for the scattering amplitude, now called *confinement induced resonance* (CIR). In what follows, we show a detailed account of a renormalization of the 3D interaction into an effective 1D interaction, which produces the CIR. This technique plays a crucial role in Sec. 5 in order to realize an integrable condition for spinor GP equations.

3.1 Model Hamiltonian

We start with the following model:

1. The trap potential is composed by an axially symmetric 2D harmonic potential of a frequency $\omega_\perp$ in the x-y plane.
2. Atomic motion for the z direction is free.
3. Interatomic interaction potential is represented by the Fermi-Huang pseudopotential:

$$v(r) = g\delta(\mathbf{r})\frac{\partial}{\partial r}(r\cdot), \tag{21}$$

   where the coupling strength g is expressed by the 3D s-wave scattering length a as eq. (7) (Meystre; 2002).
4. The energy of atoms for both transverse and longitudinal motions is well below the transverse vibrational energy $\hbar\omega_\perp$.

In the harmonic potential we can separate the center of mass and relative motion. Then we consider the Schrödinger equation for the relative motion,

$$\left[-\frac{\hbar^2}{2m_\mathrm{r}}\frac{\partial^2}{\partial z^2} + g\delta(\mathbf{r})\frac{\partial}{\partial r}(r\cdot) + \hat{H}_\perp\right]\Psi(\mathbf{r}) = E\Psi(\mathbf{r}), \tag{22}$$

where the reduced mass $m_\mathrm{r} = m/2$, the relative coordinate $\mathbf{r} = \mathbf{r}_1 - \mathbf{r}_2$, and the transverse Hamiltonian:

$$\hat{H}_\perp \equiv -\frac{\hbar^2}{2m_\mathrm{r}}\left[\frac{\partial^2}{\partial x^2} + \frac{\partial^2}{\partial y^2}\right] + \frac{m_\mathrm{r}\omega_\perp^2}{2}(x^2 + y^2). \tag{23}$$

From the above condition 4, we assume that the incident wave is factorized as $\mathrm{e}^{\mathrm{i}k_z z}\phi_{n=0,m_z=0}(r_\perp)$, where $\phi_{n=0,m_z=0}(r_\perp)$ is the transverse ground state ($r_\perp^2 \equiv x^2 + y^2$). The longitudinal kinetic energy is smaller than the energy separation between the ground state and the first axially symmetric excited state:

$$\frac{\hbar^2 k_z^2}{2m_\mathrm{r}} < E_{n=2,m_z=0} - E_{n=0,m_z=0} = 2\hbar\omega_\perp, \tag{24}$$

where $E_{n,m_z} = \hbar\omega_\perp(n+1)$ is the energy spectrum of 2D harmonic oscillator with n = 0, 1, 2, . . . the principal quantum number, and m_z the angular momentum around the z axis, which takes on values m_z = 0, 2, 4, . . . ,n (1, 3, 5, . . . ,n) for even (odd) n.

3.2 One-dimensional scattering amplitude

The asymptotic form of the scattering wave function is given by

$$\Psi(z,r_\perp) \to \left[e^{ik_z z} + f_{\text{even}} e^{ik_z|z|} + \text{sgn}(z) f_{\text{odd}} e^{ik_z|z|}\right] \phi_{0,0}(r_\perp), \quad \text{as } |z| \to \infty, \tag{25}$$

where f_{even} and f_{odd} denote the one-dimensional scattering amplitudes for the even and odd partial waves, respectively. While the transverse state ($n = m_z = 0$) remains unchanged under the assumption of low energy scattering considered above, the scattering amplitudes $f_{\text{even,odd}}$ are affected by a virtual excited state of the axially symmetric modes ($n > 0, m_z = 0$) during the collision.

To calculate the one-dimensional scattering amplitude we expand the solution,

$$\Psi(z,r_\perp) = e^{ik_z z}\phi_{0,0}(r_\perp) + \sum_{n=\text{even}} A_n e^{ik_z^{(n)}|z|}\phi_{n,0}(r_\perp), \tag{26}$$

where $\phi_{n=\text{even},0}$ is the (axially symmetric) eigenstate of the transverse Hamiltonian (23), and substitute this expansion into eq. (22) with the eigenvalue $E = \hbar^2 k_z^2/2m_r + \hbar\omega_\perp$. Operating

$$2\pi \int_0^\infty dr_\perp r_\perp \phi_{0,0}^*(r_\perp) \int_{-\varepsilon}^{\varepsilon} dz \tag{27}$$

to both side of the Schrödinger equation and taking the limit, in sequence, $\varepsilon \to 0^+$, $z \to \infty$, along with the asymptotic form (25), we can obtain $k_z^{(0)} = k_z$ and the following expression for the scattering amplitudes:

$$f_{\text{even}} \equiv A_0 = -\frac{igm_r}{\hbar^2 k_z}\phi_{0,0}^*(0)\Psi_{\text{reg}}; \quad f_{\text{odd}} = 0. \tag{28}$$

Here we have used the normalization condition:

$$2\pi \int_0^\infty dr_\perp r_\perp |\phi_{0,0}(r_\perp)|^2 = 1, \tag{29}$$

and the $r \to 0$ limit of the regular (free of the $1/r$ divergence) part of the solution Ψ,

$$\Psi_{\text{reg}} \equiv \frac{\partial}{\partial r}[r\Psi(\mathbf{r})]|_{r\to 0} = \frac{\partial}{\partial z}[z\Psi(z, r_\perp = 0)]|_{z\to 0^+}. \tag{30}$$

We note that the regularization operator $\frac{\partial}{\partial r}(r\cdot)$ that removes the $1/r$ divergence from the scattered wave plays an important role in this derivation. All the expansion coefficients A_n ($n = 2, 4, \ldots$) in eq. (26) can be obtained in the same procedure for each mode $\phi_{n,0}(r_\perp)$ with the corresponding imaginary wave number:

$$k_z^{(n)} = \frac{2i}{a_\perp}\left(\frac{n}{2} - \frac{k_z^2 a_\perp^2}{4}\right)^{1/2}, \tag{31}$$

the normalization condition of $\phi_{n,0}(r_\perp)$ and a simple relation: $|\phi_{n,0}(0)|^2 = 1/(\pi a_\perp^2)$. Here $a_\perp$ is the oscillator length of the (relative) transverse motion,

$$a_\perp = \sqrt{\frac{\hbar}{m_r\omega_\perp}}. \tag{32}$$

Recall that due to the condition (24) the value inside the parentheses in eq. (31) is positive definite. Thus, the expression for the wave function along the z axis reads

$$\Psi(z,r_\perp=0)=\frac{1}{\sqrt{\pi}a_\perp}e^{ik_z z}-\frac{igm_r}{\pi\hbar^2k_z a_\perp^2}\Psi_{reg}e^{ik_z|z|}-\frac{gm_r}{2\pi\hbar^2a_\perp}\Psi_{reg}\Lambda\left[\frac{2|z|}{a_\perp},-\left(\frac{k_z a_\perp}{2}\right)^2\right], \quad (33)$$

where the function Λ is defined as

$$\Lambda[\xi,\epsilon]=\sum_{s'=1}^{\infty}\frac{\exp(-\sqrt{s'+\epsilon}\,\xi)}{\sqrt{s'+\epsilon}}; \quad (34)$$

the sum over $s'=n/2$ originates from the sum appearing in eq. (26). We have chosen the value $\phi_{0,0}(0)$ to be real and positive. By subtracting and adding a sum,

$$\sum_{s'=1}^{\infty}\int_{s'-1}^{s'}ds''\frac{\exp(-\sqrt{s''}\,\xi)}{\sqrt{s''}}=\frac{2}{\xi}, \quad (35)$$

to the function Λ, and then, collecting ξ^0 term from the Taylor series of $\exp(-\sqrt{s''}\,\xi)$ and $\exp(-\sqrt{s''+\epsilon}\,\xi)$ with respect to ξ, one can show an expansion,

$$\Lambda[\xi,\epsilon]=\frac{2}{\xi}+\Lambda^{(0)}(\epsilon)+\Lambda^{(1)}(\epsilon)\xi+\ldots. \quad (36)$$

Here the zero-order term of the expansion has a form,

$$\Lambda^{(0)}(\epsilon)=-C+\bar{\Lambda}^{(0)}(\epsilon), \quad (37)$$

with

$$C=\lim_{s\to\infty}\left(\int_0^s\frac{ds'}{\sqrt{s'}}-\sum_{s'=1}^{s}\frac{1}{\sqrt{s'}}\right)=-\zeta(1/2)=1.4603\ldots, \quad (38)$$

and

$$\bar{\Lambda}^{(0)}(\epsilon)=\sum_{s'=1}^{\infty}\left(\frac{1}{\sqrt{s'+\epsilon}}-\frac{1}{\sqrt{s'}}\right)=\sum_{j=1}^{\infty}(-1)^j\frac{\zeta[(1+2j)/2](2j-1)!!\epsilon^j}{2^j j!}. \quad (39)$$

Substituting eq. (33) with eq. (36) into eq. (30), we get Ψ_{reg} in an explicit form.
We then write the final expression of the one-dimensional scattering amplitudes (25) as

$$f_{even}=-\frac{1}{1+ik_z a_{1D}-\underbrace{(ik_z a_\perp/2)\bar{\Lambda}^{(0)}(-k_z^2a_\perp^2/4)}_{\mathcal{O}(k_z^3a_\perp^3)}}, \quad (40)$$

with the 1D scattering length:

$$a_{1D}=-\frac{a_\perp^2}{2a}\left(1-C\frac{a}{a_\perp}\right). \quad (41)$$

3.3 Effective one-dimensional coupling strength

The expression (40) is an exact result for the potential (21) with arbitrary strength of the transverse confinement $a_\perp$. For atoms with the low kinetic energy, we can drop $\mathcal{O}(k_z^3 a_\perp^3)$ term in the denominator of the scattering amplitudes (40), obtaining a one-dimensional contact potential,

$$v_{1D}(z) = \bar{g}\delta(z), \tag{42}$$

were the coupling strength:

$$\bar{g} = -\frac{\hbar^2}{m_r a_{1D}} = \frac{4\hbar^2 a}{m a_\perp^2}\frac{1}{1 - C(a/a_\perp)}. \tag{43}$$

Note that a simple average of the three-dimensional coupling $g = 4\pi\hbar^2 a/m$ over the transverse ground state only reproduces the coefficient of (43),

$$2\pi \int_0^\infty \mathrm{d}r_\perp r_\perp |\phi_{0,0}(r_\perp)|^2 \frac{4\pi\hbar^2 a}{m}\delta(\mathbf{r}) = \frac{4\hbar^2 a}{m a_\perp^2}\delta(z). \tag{44}$$

The resonance factor $1/[1 - C(a/a_\perp)]$ implies a possibility to control the strength of atomatom scattering via tuning a confinement potential $a_\perp$. The physical origin of the CIR is attributed to a zero-energy Feshbach resonance in which the transverse modes of the confining potential assume the roles of "open" and "closed" scattering channels.

4. Spinor Bose–Einstein condensate

In this section, we extend the model of a single component condensate discussed in Sec. 2 to that of a multicomponent condensate with the spin degrees of freedom, which we call a *spinor condensate* for short (Pethick & Smith; 2002). In terms of "spin", we mean the hyperfine spin of atoms in this chapter.

4.1 Hamiltonian

The hyperfine spin f is defined by $f = s + i$, where s and i denote the electronic and nuclear spins of the atoms. For simplicity, we consider bosons with the hyperfine spin $f = 1$. This includes alkalis with nuclear spin $i = 3/2$ such as ^{7}Li, ^{87}Rb, and ^{23}Na. Alkali bosons with $f > 1$ such as ^{85}Rb (with $i = 5/2$), and ^{133}Cs (with $i = 7/2$) may have even richer structures.
Atoms in the $f = 1$ state are characterized by a vectorial field operator with the components subject to the hyperfine spin manifold. The three-component field $\hat{\Psi} = \{\hat{\Psi}_1, \hat{\Psi}_0, \hat{\Psi}_{-1}\}^T$, where the superscript T denotes the transpose, satisfies the bosonic commutation relations:

$$[\hat{\Psi}_\alpha(\mathbf{r},t), \hat{\Psi}_\beta^\dagger(\mathbf{r}',t)] = \delta_{\alpha,\beta}\delta(\mathbf{r} - \mathbf{r}'). \tag{45}$$

In order to discuss the properties of spinor Bose gases, we start with the following second quantized Hamiltonian,

$$\hat{H} = \hat{H}_0 + \hat{H}_{\mathrm{int}} + \hat{H}_{lz} \tag{46}$$

$$\hat{H}_0 = \int \mathrm{d}\mathbf{r} \sum_\alpha \hat{\Psi}_\alpha^\dagger(\mathbf{r},t)\left[-\frac{\hbar^2}{2m}\nabla^2 + U_{\mathrm{trap}}(\mathbf{r})\right]\hat{\Psi}_\alpha(\mathbf{r},t), \tag{47}$$

$$\hat{H}_{\text{int}} = \frac{1}{2}\int \mathrm{d}\mathbf{r}\int \mathrm{d}\mathbf{r}' \sum_{\alpha,\alpha',\beta,\beta'} \hat{\Psi}^{\dagger}_{\alpha}(\mathbf{r},t)\hat{\Psi}^{\dagger}_{\beta}(\mathbf{r}',t)v(\mathbf{r}-\mathbf{r}')_{\alpha\alpha'\beta\beta'}\hat{\Psi}_{\alpha'}(\mathbf{r},t)\hat{\Psi}_{\beta'}(\mathbf{r}',t), \tag{48}$$

$$\hat{H}_{lz} = -p\int \mathrm{d}\mathbf{r}\sum_{\alpha,\beta}\hat{\Psi}^{\dagger}_{\alpha}(\mathbf{r},t)f^{z}_{\alpha,\beta}\hat{\Psi}_{\beta}(\mathbf{r},t) \tag{49}$$

where $U_{\text{trap}}(\mathbf{r})$ is the external trap potential, $v(\mathbf{r} - \mathbf{r}')$ expresses the two-body interaction and subscripts $\{\alpha, \beta, \alpha', \beta' = 1, 0, -1\}$ denote the components of the spin. The last term in eq. (46), $\hat{H}_{lz}$, is the response to an external magnetic field p (the linear Zeeman effect). This response to the magnetic field necessarily selects one of several possible ground states, or the so-called weak field seeking state, $m_f = -1$ for $f = 1$ case where the spin degrees of freedom are "frozen". We set $p = 0$ throughout this chapter.

Due to the Bose–Einstein statistics, the total spin $F = f_1 + f_2$ of any two bosons whose relative orbital angular momentum is zero should be restricted to even, $F = 2f, 2f-2, \ldots, 0$. Thus, the interatomic interaction $\hat{v}(\mathbf{r} - \mathbf{r}')$ can be divided into several sectors labeled by F as

$$\hat{v}(\mathbf{r}-\mathbf{r}') = \delta(\mathbf{r}-\mathbf{r}')\sum_{F=\text{even}} g_F\hat{P}_F, \tag{50}$$

where $\hat{P}_F$ is the projection operator and g_F characterizes the strength of the binary interaction between bosonic atoms with the total spin F. This coupling constant g_F is related to the corresponding s-wave scattering length a_F as

$$g_F = \frac{4\pi\hbar^2 a_F}{m}. \tag{51}$$

For $f = 1$ bosons, since F takes only on values 0 and 2, we can rewrite the potential $\hat{v}(\mathbf{r} - \mathbf{r}')$ in a simple form using the following two properties of the projection operators $\hat{P}_0, \hat{P}_2$; the completeness of the operators,

$$\hat{P}_0 + \hat{P}_2 = \hat{I}, \tag{52}$$

where $\hat{I}$ is an identity operator, and the product of the angular momentum operators,

$$\hat{\mathbf{f}}\cdot\hat{\mathbf{f}}' = \frac{1}{2}\left[\hat{\mathbf{F}}^2 - \hat{\mathbf{f}}^2 - \hat{\mathbf{f}}'^2\right] = \sum_{F=0,2}\frac{1}{2}[F(F+1) - 2f(f+1)]\hat{P}_F = \hat{P}_2 - 2\hat{P}_0, \tag{53}$$

where a hat "^" on $\mathbf{f}$ means an operator as projection. Solving these equations (52), (53) for $\hat{P}_0$ and $\hat{P}_2$, we obtain the form of the interaction in terms of the angular momentum operators,

$$\hat{v}(\mathbf{r}-\mathbf{r}') = \delta(\mathbf{r}-\mathbf{r}')(c_0\hat{I} + c_1\hat{\mathbf{f}}_1\cdot\hat{\mathbf{f}}_2). \tag{54}$$

In this expression,

$$c_0 = \frac{2g_2 + g_0}{3}, \qquad c_1 = \frac{g_2 - g_0}{3}, \tag{55}$$

which are the magnitude of the density-density interaction and of the spin-spin interaction, respectively. Thus, the interaction Hamiltonian is rewritten as

$$\hat{H}_{\rm int} = \frac{c_0}{2}\int d\mathbf{r}\sum_{\alpha,\beta}\hat{\Psi}^\dagger_\alpha(\mathbf{r},t)\hat{\Psi}^\dagger_\beta(\mathbf{r},t)\hat{\Psi}_\alpha(\mathbf{r},t)\hat{\Psi}_\beta(\mathbf{r},t) + \frac{c_1}{2}\int d\mathbf{r}\sum_{\alpha,\alpha',\beta,\beta'}\hat{\Psi}^\dagger_\alpha(\mathbf{r},t)\hat{\Psi}^\dagger_\beta(\mathbf{r},t)\mathbf{f}_{\alpha\beta}\cdot\mathbf{f}_{\alpha'\beta'}\hat{\Psi}_{\alpha'}(\mathbf{r},t)\hat{\Psi}_{\beta'}(\mathbf{r},t), \tag{56}$$

where we may use the following expressions of spin-1 matrices $\mathbf{f} = (f^x, f^y, f^z)$ as

$$f^x = \frac{1}{\sqrt{2}}\begin{pmatrix}0&1&0\\1&0&1\\0&1&0\end{pmatrix},\quad f^y = \frac{i}{\sqrt{2}}\begin{pmatrix}0&-1&0\\1&0&-1\\0&1&0\end{pmatrix},\quad f^z = \begin{pmatrix}1&0&0\\0&0&0\\0&0&-1\end{pmatrix}. \tag{57}$$

A construction of the interaction Hamiltonian for a general hyperfine spin f can be found in (Ueda & Koashi; 2002).

4.2 $f = 1$ spinor condensate in quasi 1D regime

From now on, we assume that the system is quasi-one dimensional: the trapping potential is suitably anisotropic such that the transverse spatial degrees of freedom (y-z plain) is factorized from the longitudinal (x axis) and all the hyperfine states are in transverse ground state.

As derived in Sec. 2, in the mean-field theory of the spinor BEC, the assembly of atoms in the $f = 1$ state is characterized by a vectorial order parameter:

$$\Phi(x,t) \equiv [\Phi_1(x,t), \Phi_0(x,t), \Phi_{-1}(x,t)]^T \tag{58}$$

where the subscripts {1, 0,–1} denote the magnetic quantum numbers with the components subject to the hyperfine spin space. The normalization is imposed as

$$\int dx\,\Phi(x,t)^\dagger\cdot\Phi(x,t) = N_{\rm T}, \tag{59}$$

where N_T is the total number of atoms.

According to the discussion in Sec. 3, the effective 1D couplings $\bar{g}_0$ and $\bar{g}_2$ are represented by

$$\bar{g}_F = \frac{4\hbar^2 a_F}{m a_\perp^2}\frac{1}{1 - C(a_F/a_\perp)}, \tag{60}$$

where a_F is the 3D s-wave scattering length of the total hyperfine spin F = 0, 2 channels, respectively, and $a_\perp$ is the size of the ground state in the (relative) transverse motion.

Thus, the Gross-Pitaevskii energy functional of this system is given by

$$E_\Phi = \int dx\left\{\Phi^*_\alpha(x,t)\left[-\frac{\hbar^2}{2m}\partial_x^2\right]\Phi_\alpha(x,t) + \frac{\bar{c}_0}{2}n^2(x,t) + \frac{\bar{c}_1}{2}\mathbf{f}^2(x,t)\right\}, \tag{61}$$

with the particle number and spin densities, respectively, defined by

$$n(x,t) \equiv \Phi^*_\alpha(x,t)\Phi_\alpha(x,t), \qquad \mathbf{f}(x,t) \equiv \Phi^*_\alpha(x,t)\mathbf{f}_{\alpha\beta}\Phi_\beta(x,t). \tag{62}$$

The coupling constants $\bar{c}_0$ and $\bar{c}_1$ are connected to those in eqs. (60) (cf. eq. (43)) as

$$\bar{c}_0 = \frac{2\bar{g}_2 + \bar{g}_0}{3}, \qquad \bar{c}_1 = \frac{\bar{g}_2 - \bar{g}_0}{3}. \tag{63}$$

The time-evolution of spinor condensate wave function $\Phi(x, t)$ can be derived from

$$\mathrm{i}\hbar\partial_t \Phi_\alpha(x,t) = \frac{\delta E_\Phi}{\delta \Phi_\alpha^*(x,t)}. \tag{64}$$

Substituting eq. (61) into eq. (64), we get a set of equations for the longitudinal wave functions of the spinor condensate:

$$\begin{aligned}\mathrm{i}\hbar\partial_t \Phi_1(x,t) = &-\frac{\hbar^2}{2m}\partial_x^2 \Phi_1(x,t) + (\bar{c}_0 + \bar{c}_1)\left[|\Phi_1(x,t)|^2 + |\Phi_0(x,t)|^2\right]\Phi_1(x,t) \\ &+ (\bar{c}_0 - \bar{c}_1)|\Phi_{-1}(x,t)|^2\Phi_1(x,t) + \bar{c}_1\Phi_{-1}^*(x,t)\Phi_0^2(x,t),\end{aligned} \tag{65a}$$

$$\begin{aligned}\mathrm{i}\hbar\partial_t \Phi_0(x,t) = &-\frac{\hbar^2}{2m}\partial_x^2 \Phi_0(x,t) + (\bar{c}_0 + \bar{c}_1)\left[|\Phi_1(x,t)|^2 + |\Phi_{-1}(x,t)|^2\right]\Phi_0(x,t) \\ &+ \bar{c}_0|\Phi_0(x,t)|^2\Phi_0(x,t) + 2\bar{c}_1\Phi_0^*(x,t)\Phi_1(x,t)\Phi_{-1}(x,t),\end{aligned} \tag{65b}$$

$$\begin{aligned}\mathrm{i}\hbar\partial_t \Phi_{-1}(x,t) = &-\frac{\hbar^2}{2m}\partial_x^2 \Phi_{-1}(x,t) + (\bar{c}_0 + \bar{c}_1)\left[|\Phi_{-1}(x,t)|^2 + |\Phi_0(x,t)|^2\right]\Phi_{-1}(x,t) \\ &+ (\bar{c}_0 - \bar{c}_1)|\Phi_1(x,t)|^2\Phi_{-1}(x,t) + \bar{c}_1\Phi_1^*(x,t)\Phi_0^2(x,t).\end{aligned} \tag{65c}$$

5. Integrable model

To analyze the dynamical properties of the coupled system (65), we propose an integrable model as follows (Ieda et al.; 2004a,b). We consider the system with the coupling constants,

$$\bar{c}_0 = \bar{c}_1 \equiv -c < 0, \qquad (2\bar{g}_0 = -\bar{g}_2 > 0). \tag{66}$$

This situation corresponds to attractive mean-field interaction $\bar{c}_0 < 0$ and ferromagnetic spin-exchange interaction $\bar{c}_1 < 0$. Note that in preceding investigations of spinor condensates (Pethick & Smith; 2002), mean-field interaction is assumed to be repulsive $c_0 > 0$ and far exceeding spin-exchange interaction in the magnitude $c_0 \gg |c_1|$ in line with experimental data. Thus, the parameter regime (66) was not been explored in detail.

The effective interactions between atoms in a BEC have been tuned with a Feshbach resonance (Pethick & Smith; 2002). In spinor BECs, however, we should extend this to alternative techniques such as an optically induced Feshbach resonance or a confinement induced resonance (Olshanii; 1998), which do not affect the rotational symmetry of the internal spin states. In the latter, the above condition is surely obtained by setting

$$a_\perp = 3\mathrm{C}\frac{a_0 a_2}{2a_0 + a_2}, \tag{67}$$

in eq. (60) when

$$a_0 > a_2 > 0 \qquad \text{or} \qquad a_2 > 0 > a_0. \tag{68}$$

It is worth noting that the integrable property itself is independent of the sign of $\bar{c}_0$ ($\bar{c}_1$) as far as their magnitudes are equal to each other. The opposite sign case, i.e., $\bar{c}_0 = \bar{c}_1 \equiv c > 0$, can be analyzed in the same manner (Uchiyama et al.; 2006).
In the dimensionless form:

$$\mathbf{\Phi} \to \{\phi_1, \sqrt{2}\phi_0, \phi_{-1}\}^T, \tag{69}$$

where time and length are measured in units of

$$\bar{t} = \frac{\hbar a_\perp}{c}, \qquad \bar{x} = \hbar\sqrt{\frac{a_\perp}{2mc}}, \tag{70}$$

respectively, we rewrite eqs. (65) as follows, (we omit the arguments (x, t) hereafter.)

$$\mathrm{i}\partial_t\phi_1 = -\partial_x^2\phi_1 - 2\{|\phi_1|^2 + 2|\phi_0|^2\}\phi_1 - 2\phi_{-1}^*\phi_0^2, \tag{71a}$$

$$\mathrm{i}\partial_t\phi_0 = -\partial_x^2\phi_0 - 2\{|\phi_{-1}|^2 + |\phi_0|^2 + |\phi_1|^2\}\phi_0 - 2\phi_0^*\phi_1\phi_{-1}, \tag{71b}$$

$$\mathrm{i}\partial_t\phi_{-1} = -\partial_x^2\phi_{-1} - 2\{|\phi_{-1}|^2 + 2|\phi_0|^2\}\phi_{-1} - 2\phi_1^*\phi_0^2. \tag{71c}$$

Now we find that these coupled equations (71) are equivalent to a 2×2 matrix version of nonlinear Schrödinger (NLS) equation:

$$\mathrm{i}\partial_t Q + \partial_x^2 Q + 2QQ^\dagger Q = O, \tag{72}$$

with an identification,

$$Q = \begin{pmatrix} \phi_1 & \phi_0 \\ \phi_0 & \phi_{-1} \end{pmatrix}. \tag{73}$$

Since the matrix NLS equation (72) is completely integrable (Tsuchida & Wadati; 1998), the integrability of the reduced equations (71) are proved automatically (Ieda et al.; 2004a). Remark that the general $M\times L$ matrix NLS equation is also integrable. It is worthy to search other integrable models for higher spin case (Uchiyama et al.; 2007).

5.1 Soliton solution

We summarize an explicit formula for the soliton solution of the 2 × 2 matrix version of NLS equation (72) with eq. (73) by considering a reduction of a general formula obtained in (Tsuchida & Wadati; 1998).
Under the vanishing boundary condition, one can apply the inverse scattering method (ISM) to the nonlinear time evolution equation (72) associated with the generalized Zakharov-Shabat eigenvalue problem:

$$\partial_x \begin{bmatrix} \Psi_1 \\ \Psi_2 \end{bmatrix} = \frac{1}{2}\begin{bmatrix} k^* I & 2Q \\ -2Q^\dagger & -k^* I \end{bmatrix}\begin{bmatrix} \Psi_1 \\ \Psi_2 \end{bmatrix}. \tag{74}$$

Here Ψ_1 and Ψ_2 take their values in 2 × 2 matrices. The complex number k is the spectral parameter. I is the 2 × 2 unit matrix. The 2 × 2 matrix Q plays a role as a potential function in this linear system. According to (Tsuchida & Wadati; 1998), N-soliton solution of eq. (72) with eq. (73) is expressed as

$$Q(x,t) = (\underbrace{I\,I\cdots I}_{N})S^{-1}\begin{bmatrix}\Pi_1 e^{\chi_1}\\ \Pi_2 e^{\chi_2}\\ \vdots\\ \Pi_N e^{\chi_N}\end{bmatrix}, \tag{75}$$

where the $2N \times 2N$ matrix S is given by

$$S_{ij} = \delta_{ij}I + \sum_{l=1}^{N}\frac{\Pi_i \cdot \Pi_l^{\dagger}}{(k_i + k_l^*)(k_j + k_l^*)}e^{\chi_i+\chi_l^*}, \qquad 1 \le i,j \le N. \tag{76}$$

Here we have introduced the following parameterizations:

$$\Pi_j = \begin{pmatrix}\beta_j & \alpha_j\\ \alpha_j & \gamma_j\end{pmatrix}, \tag{77}$$

$$\chi_j \equiv \chi_j(x,t) = k_j x + ik_j^2 t - \epsilon_j. \tag{78}$$

The 2 × 2 matrices Π_j normalized to unity in a sense of the square norm,

$$||\Pi_j||_2 \equiv \sqrt{2|\alpha_j|^2 + |\beta_j|^2 + |\gamma_j|^2} = 1, \tag{79}$$

must take the same form as Q from their definition. We call them "polarization matrices," which determine both the populations of three components {1, 0, –1} within each soliton and the relative phases between them. The complex constants k_j denote discrete eigenvalues, each of which determines a bound state by the potential Q. ϵ_j are real constants which can be used to tune the initial displacements of solitons. It is worth noting that all x and t dependence is only through the variables $\chi_j(x, t)$. As we shall see in Sec. 6, the real part of $\chi_j(x, t)$ represents the coordinate for observing soliton-j's envelope while the imaginary part of it represents the coordinate for observing soliton-j's carrier waves.

The same procedure can be performed for nonvanishing boundary conditions (Ieda et al.; 2007) which is relevant to formation of spinor dark solitons (Uchiyama et al.; 2006).

Equation (72) is a completely integrable system whose initial value problems can be solved via, for example, the ISM (Tsuchida & Wadati; 1998) (Ieda et al.; 2007). The existence of the **r**-matrix for this system guarantees the existence of an infinite number of conservation laws which restrict the dynamics of the system in an essential way. Here we show explicit forms of some conserved quantities, i.e., total number, total spin (magnetization), total momentum and total energy.

$$\textbf{total number:} \quad N_{\mathrm{T}} = \int \mathrm{d}x\, n(x,t); \tag{80}$$

$$n(x,t) = \Phi^{\dagger}\cdot\Phi = \mathrm{tr}\{Q^{\dagger}Q\}. \tag{81}$$

$$\textbf{total spin:} \quad \mathbf{F}_{\mathrm{T}} = \int \mathrm{d}x\, \mathbf{f}(x,t); \tag{82}$$

$$\mathbf{f}(x,t) = \Phi^{\dagger} \cdot \mathbf{f} \cdot \Phi = \mathrm{tr}\{Q^{\dagger}\boldsymbol{\sigma} Q\}. \tag{83}$$

$$\textbf{total momentum:} \quad P_{\mathrm{T}} = \int \mathrm{d}x\, p(x,t); \tag{84}$$

$$p(x,t) = -\mathrm{i}\hbar\Phi^{\dagger} \cdot \partial_x \Phi = -\mathrm{i}\hbar \cdot \mathrm{tr}\{Q^{\dagger} Q_x\}. \tag{85}$$

$$\textbf{total energy:} \quad E_{\mathrm{T}} = \int \mathrm{d}x\, e(x,t); \tag{86}$$

$$e(x,t) = \frac{\hbar^2}{2m}\partial_x\Phi^{\dagger} \cdot \partial_x\Phi - \frac{c}{2}\left[n(x,t)^2 + \mathbf{f}(x,t)^2\right] = c \cdot \mathrm{tr}\{Q_x^{\dagger}Q_x - Q^{\dagger}QQ^{\dagger}Q\}. \tag{87}$$

Here tr{·} denotes the matrix trace and $\boldsymbol{\sigma} = (\sigma^x, \sigma^y, \sigma^z)^T$ are the Pauli matrices,

$$\sigma^x = \begin{pmatrix} 0 & 1 \\ 1 & 0 \end{pmatrix}, \quad \sigma^y = \begin{pmatrix} 0 & -\mathrm{i} \\ \mathrm{i} & 0 \end{pmatrix}, \quad \sigma^z = \begin{pmatrix} 1 & 0 \\ 0 & -1 \end{pmatrix}. \tag{88}$$

6. Spin property of one-soliton solution

In this section, we discuss one-soliton solutions and classify them by their spin states. If we set $N = 1$ in the formula (75) we obtain the one-soliton solution:

$$Q = \frac{\mathrm{e}^{\chi}}{\det S}\begin{pmatrix} \beta + \gamma^* \mathrm{e}^{2\chi_{\mathrm{R}}+\rho}\det\Pi & \alpha - \alpha^* \mathrm{e}^{2\chi_{\mathrm{R}}+\rho}\det\Pi \\ \alpha - \alpha^* \mathrm{e}^{2\chi_{\mathrm{R}}+\rho}\det\Pi & \gamma + \beta^* \mathrm{e}^{2\chi_{\mathrm{R}}+\rho}\det\Pi \end{pmatrix}, \tag{89}$$

where

$$\det S = 1 + \mathrm{e}^{2\chi_{\mathrm{R}}+\rho} + \mathrm{e}^{4\chi_{\mathrm{R}}+2\rho}|\det\Pi|^2, \qquad \mathrm{e}^{\rho/2} \equiv \frac{1}{2k_{\mathrm{R}}}, \qquad \Pi \equiv \begin{pmatrix} \beta & \alpha \\ \alpha & \gamma \end{pmatrix}, \tag{90}$$

$$\chi_{\mathrm{R}} \equiv \chi_{\mathrm{R}}(x,t) = k_{\mathrm{R}}(x - 2k_{\mathrm{I}}t) - \epsilon, \qquad \chi_{\mathrm{I}} \equiv \chi_{\mathrm{I}}(x,t) = k_{\mathrm{I}}x + (k_{\mathrm{R}}^2 - k_{\mathrm{I}}^2)t. \tag{91}$$

We have omitted the subscripts of the soliton number. Here and hereafter, the subscripts R and I denote real and imaginary parts, respectively. Throughout this section, we set $k_R > 0$ without loss of generality. We remark the significance of each parameter/coordinate as follows,

Π : polarization matrix of soliton
k_{R} : amplitude of soliton
$2k_{\mathrm{I}}$: velocity of soliton's envelope
χ_{R} : coordinate for observing soliton's envelope
χ_{I} : coordinate for observing soliton's carrier wave.

We use the term "amplitude" to indicate the peak(s) height of soliton's envelope. Actual amplitude should be represented as k_{R} multiplied by a factor from 1 to $\sqrt{2}$ which is

determined by the type of polarization matrices. The explicit form will be shown later. As mentioned before, soliton's motion depends on both x and t via variables χ_R and χ_I, from which we can see the meaning of velocity of soliton.
From a total spin conservation, one-soliton solution can be classified by the spin states. We shall show that the only two spin states are allowable,

$$\mathbf{F}_T = (0,0,0)^T \qquad \text{for} \qquad \det\Pi \neq 0, \tag{92a}$$

$$|\mathbf{F}_T| = N_T \qquad \text{for} \qquad \det\Pi = 0. \tag{92b}$$

Substituting eqs. (89)–(91) into eq. (83), we obtain the local spin density of the one-soliton solution:

$$\mathbf{f}(x,t) = \frac{e^{2\chi_R}}{(\det S)^2}\left(1 - e^{4\chi_R+2\rho}|\det\Pi|^2\right)\mathrm{tr}\{\Pi^\dagger\boldsymbol{\sigma}\Pi\}. \tag{93}$$

We also give the explicit form of the number density:

$$n(x,t) = \frac{e^{2\chi_R}}{(\det S)^2}\left\{1 + \left(4e^{2\chi_R+\rho} + e^{4\chi_R+2\rho}\right)|\det\Pi|^2\right\}. \tag{94}$$

To clarify the physical meaning of detΠ, we define here another important local density as

$$\Theta(x,t) \equiv \Phi_0^2 - 2\Phi_1\Phi_{-1} = -2\det Q. \tag{95}$$

This quantity measures the formation of singlet pairs. Note that these "pairs" are distinguished from Cooper pairs of electrons or those of ^{3}He owing to the different statistical properties of ingredient particles. Since $\Theta(x, t)$ does not contribute to the magnetization of the soliton, it is invariant under any spin rotation. As far as ground state properties are concerned, it is not necessary to introduce $\Theta(x, t)$ for a system of spin-1 bosons, while a counterpart to eq. (95) plays a crucial role for spin-2 case (Ueda & Koashi; 2002). As we shall show later, however, it is useful to characterize solitons within energy degenerated states.
In the case of the one-soliton solution (89), the singlet pair density is proportional to the determinant of the polarization matrix Π,

$$\Theta(x,t) = -2\frac{e^{2\chi}}{\det S}\det\Pi. \tag{96}$$

This suggests that detΠ represents the magnitude of the singlet pairs. For the general N-soliton case, this singlet pair density can vary after each collision of solitons and is not the conserved density. The detail will be discussed at the end of this section.
In what follows, we classify spin states of the one-soliton solution based on the values of detΠ.

6.1 Ferromagnetic state

Let detΠ = 0, then eq. (89) becomes a simple form:

$$Q = k_R\,\mathrm{sech}(\chi_R + \rho/2)\Pi e^{i\chi_I}. \tag{97}$$

Now all of m_F = 0, ±1 components share the same wave function. Their distribution in the internal state reflects directly the elements of the polarization matrix Π. One can see the meaning of each parameter listed above. By definition, the singlet pair density (96) vanishes everywhere. Thus, this type of soliton belongs to the *ferromagnetic* state and will be referred to as a ferromagnetic soliton. The total number of atoms is given by integrating eq. (94) as

$$N_{\mathrm{T}} = 2k_{\mathrm{R}}. \tag{98}$$

The total magnetization (82) becomes

$$\mathbf{F}_{\mathrm{T}} = 2k_{\mathrm{R}}\left(2\mathrm{Re}\{\alpha^*(\beta+\gamma)\}, -2\mathrm{Im}\{\alpha^*(\beta-\gamma)\}, |\beta|^2 - |\gamma|^2\right)^T, \tag{99}$$

with the modulus, $|\mathbf{F}_{\mathrm{T}}| = N_{\mathrm{T}}$. Equation (99) is connected to $\mathbf{F}'_{\mathrm{T}} = 2k_{\mathrm{R}}(0,0,1)^T$ through a gauge transformation and a spin rotation.

Next, we calculate the total momentum and the total energy of the ferromagnetic soliton. Substituting eq. (97) into eqs. (84), (86) and using detΠ = 0, we obtain

$$P_{\mathrm{T}}^{\mathrm{f}} = N_{\mathrm{T}}\hbar k_{\mathrm{I}}, \qquad E_{\mathrm{T}}^{\mathrm{f}} = N_{\mathrm{T}}c\left(k_{\mathrm{I}}^2 - \frac{k_{\mathrm{R}}^2}{3}\right), \tag{100}$$

respectively. In infinite homogeneous 1D space as considered here, it can be shown that a single component GP equation for BEC with attractive interactions, i.e., the self-focusing NLS equation possesses the one-soliton solution that minimizes the total energy for fixed number of particles and total momentum. This remains true for the spinor GP equations (71). As we will see later, for given number of N_{T}, the stationary (k_{I} = 0) one-soliton solution in the ferromagnetic state is the ground state of this system. On the other hand, in finite 1D space case, the ground state is subject to a quantum phase transition between uniform and soliton states (Kanamoto et al.; 2002).

6.2 Polar state

If detΠ ≠ 0, the local spin density has one node, i.e., $\mathbf{f}(x_0, t)$ = 0 at a point:

$$x_0 = 2k_{\mathrm{I}}t + \frac{1}{2k_{\mathrm{R}}}\left(\ln\frac{4k_{\mathrm{R}}^2}{|\det\Pi|} + 2\epsilon\right), \tag{101}$$

for each moment t. Setting $x' = x - x_0$ and $A^{-1} \equiv 2\,|\det\Pi\,|$, we get

$$\mathbf{f}(x') = -\frac{4k_{\mathrm{R}}^2 A\sinh(2k_{\mathrm{R}}x')}{\left[\cosh(2k_{\mathrm{R}}x') + A\right]^2}\begin{pmatrix} 2\mathrm{Re}\{\alpha^*(\beta+\gamma)\} \\ -2\mathrm{Im}\{\alpha^*(\beta-\gamma)\} \\ |\beta|^2 - |\gamma|^2 \end{pmatrix}. \tag{102}$$

Since each component of the local spin density is an odd function of x', its average value is zero,

$$\mathbf{F}_{\mathrm{T}} = \int \mathrm{d}x'\,\mathbf{f}(x') = (0,0,0)^T. \tag{103}$$

This implies that this type of soliton, on the average, belongs to the *polar* state (Pethick & Smith; 2002). Let us also rewrite the number density (94) as

$$n(x') = \frac{4k_{\mathrm{R}}^2 \left[A\cosh 2k_{\mathrm{R}}x' + 1\right]}{\left[\cosh 2k_{\mathrm{R}}x' + A\right]^2}. \tag{104}$$

To elaborate on this type of soliton, we further divide into two cases.
(i) $A^{-1} = 2|\det\Pi| = 1$ ($\alpha\beta^* + \alpha^*\gamma = 0$).
Under this constraint, we find the local spin (102) vanishes everywhere. Solitons in this state possess the symmetry of polar state locally. We, therefore, refer to only those solitons as polar solitons. Considering eq. (89) with the above condition, we recover a normal sech-type soliton solution:

$$Q = \sqrt{2}k_{\mathrm{R}}\mathrm{sech}(k_{\mathrm{R}}x')\Pi \mathrm{e}^{\mathrm{i}\chi_{\mathrm{I}}}. \tag{105}$$

Note that the amplitude of soliton is different from that of the ferromagnetic soliton, which leads to a relation between the total number and the spectral parameter as

$$N_{\mathrm{T}} = 4k_{\mathrm{R}}. \tag{106}$$

The total momentum and the total energy are given by

$$P_{\mathrm{T}}^{\mathrm{p}} = N_{\mathrm{T}}\hbar k_{\mathrm{I}}, \qquad E_{\mathrm{T}}^{\mathrm{p}} = N_{\mathrm{T}}c\left(k_{\mathrm{I}}^2 - \frac{k_{\mathrm{R}}^2}{3}\right), \tag{107}$$

respectively. The difference between ferromagnetic soliton energy and polar soliton energy with the same number of atoms N_T is

$$E_{\mathrm{T}}^{\mathrm{f}} - E_{\mathrm{T}}^{\mathrm{p}} = -\frac{N_{\mathrm{T}}^3 c}{16} < 0, \tag{108}$$

which is a natural consequence of the ferromagnetic interaction, i.e., $\bar{c}_1 = -c < 0$.
(ii) $A^{-1} = 2|\det\Pi| < 1$.
In this case, the local spin retains nonzero value, although the average spin amounts to be zero. The density profile (104) has the following structure. When $A > 2$, a peak of the density splits into two (Fig. 1) due to different density profiles of $m_F = 0, \pm 1$ components.
For a large value of A, namely, when $\det\Pi$ gets close to zero, such twin peaks separate away. In consequence, they behave as if a pair of two distinct ferromagnetic solitons with antiparallel spins, traveling in parallel with the same velocity and the amplitudes half as much as that of the polar soliton ($A = 1$) in the density profile [see the inset of Fig. 1(a) and Fig. 1 (b)].
Hence, solitons of this type will be referred to as split solitons. The total number is the same as the case (i),

$$N_{\mathrm{T}} = 4k_{\mathrm{R}}. \tag{109}$$

The total momentum and the total energy are the same values as those in the case (i):

$$P_{\mathrm{T}}^{\mathrm{s}} = N_{\mathrm{T}}\hbar k_{\mathrm{I}}, E_{\mathrm{T}}^{\mathrm{s}} = N_{\mathrm{T}}c\left(k_{\mathrm{I}}^2 - \frac{k_{\mathrm{R}}^2}{3}\right). \tag{110}$$

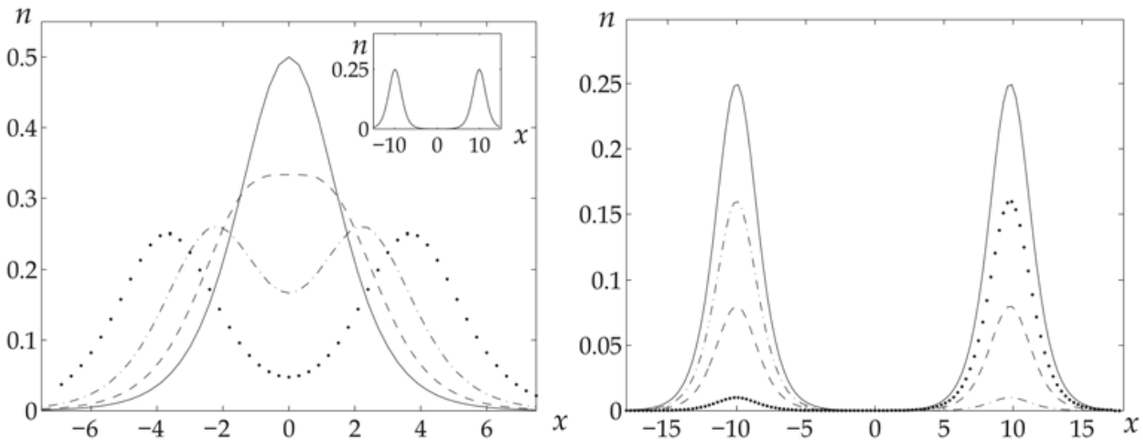

(a) (b)

Fig. 1. The density profiles of eq. (104). (a)We set $k_R = 0.5$, and $A = 1$ (solid line), 2 (dashed line), 5 (dash-dot line), 20 (dotted line). The inset shows a split soliton for $A = 10^4$, consisting of two ferromagnetic like solitons with the same velocity. (b) The density profiles of eq. (104) (solid line) for $k_R = 0.5$ and $A = 10^4$, and the three components, $m_F = 0$ (dashed line), $m_F = 1$ (dotted line) and $m_F = -1$ (dash-dot line) are shown simultaneously.

This degeneracy is ascribed to the integrable condition for the coupling constants, i.e., $\bar{c}_0 = \bar{c}_1$. Comparing case (i) with case (ii), we find that a variety of dissimilar shaped solitons are degenerated in the polar state. To characterize them, we can use, instead of A, a physical quantity defined as

$$\mathcal{S} \equiv \int \mathrm{d}x |\Theta(x,t)| = N_T \frac{2\tan^{-1}\left(\sqrt{\frac{A-1}{A+1}}\right)}{\sqrt{A^2-1}}, \tag{111}$$

which is a monotone decreasing function of $A \in [1, \infty)$; the maximum value, N_T, at $A = 1$ (polar soliton) and limiting to 0 at $A \to \infty$ (ferromagnetic soliton). In this sense, $\mathcal{S}$ has the meaning as the "total singlet pairs" of the whole system. As noted above, $\mathcal{S}$ is not the conserved quantity in general ($N \geq 2$); all the conserved densities should be expressed by the matrix trace of products of $Q^\dagger$, Q and their derivatives (Tsuchida & Wadati; 1998) as eqs. (81), (83), (85), and (87) while $|\Theta(x, t)|$ is not. Nevertheless, $\mathcal{S}$ can be used to label solitons in the polar state because it dose not change in the meanwhile prior to the subsequent collision.

7. Two-soliton collision and spin dynamics

In this section, we analyze two-soliton collisions in the spinor model. The two-soliton solutions can be obtained by setting $N = 2$ in eq. (75). The derivation is straightforward but rather lengthy. An explicit expression of the two-soliton solution is given in Appendix of (Ieda et al.; 2004b) and, here, compute asymptotic forms of specific two-soliton solutions as $t \to \mp\infty$, which define the collision properties of two-soliton in the spinor model.

For simplicity, we restrict the spectral parameters to regions:

$$k_{1R} > 0, \qquad k_{2R} < 0, \qquad k_{1I} < 0, \qquad k_{2I} > 0. \tag{112a}$$

Under the conditions, we calculate the asymptotic forms in the final state ($t\to\infty$) from those in the initial state ($t\to-\infty$). Since each soliton's envelope is located around $x \simeq 2k_{j\mathrm{I}}t$, soliton-1 and soliton-2 are initially isolated at $x \to \pm\infty$, and then, travel to the opposite directions at a velocity of $2k_{1\mathrm{I}}$ and $2k_{2\mathrm{I}}$, respectively. After a head-on collision, they pass through without changing their velocities and arrive at $x\to\mp\infty$ in the final state. Collisional effects appear not only as usual phase shifts of solitons but also as a rotation of their polarization.
According to the classification of one-soliton solutions in the previous section, we choose the following three cases: i) Polar-polar solitons collision, ii) Polar-ferromagnetic solitons collision, iii) Ferromagnetic-ferromagnetic solitons collision. As we shall see later, the polar soliton dose not affect the polarization of the other solitons apart from the total phase factor. On the other hand, ferromagnetic solitons can 'rotate' their partners' polarization, which allows for switching among the internal states.

7.1 Polar-polar solitons collision

We first deal with a collision between two polar solitons defined by k_j and Π_j (j = 1, 2) with the conditions (112) and $\alpha_j\beta_j^* + \alpha_j^*\gamma_j = 0$, equivalently,

$$|\det\Pi_1| = |\det\Pi_2| \equiv \frac{1}{2}. \tag{113}$$

In the asymptotic regions, we can consider each soliton separately. Thus, the initial state is given by the sum of two polar solitons as

$$Q \simeq Q_1^{\mathrm{in}} + Q_2^{\mathrm{in}}, \tag{114}$$

where the asymptotic form of soliton-j (j = 1, 2) is

$$Q_j^{\mathrm{in}} = \sqrt{2}k_{j\mathrm{R}}\mathrm{sech}(\chi_{j\mathrm{R}} + \rho_j/2)\Pi_j e^{\mathrm{i}\chi_{j\mathrm{I}}}. \tag{115a}$$

These can be proved by taking the limit $\chi_{2\mathrm{R}} \to -\infty$ with keeping $\chi_{1\mathrm{R}}$ finite and, vice versa, $\chi_{1\mathrm{R}} \to -\infty$ with $\chi_{2\mathrm{R}}$ fixed. Phase factors which come from the values of $|\det\Pi_j|$ are absorbed by the arbitrary constants ϵ_j inside $\chi_{j\mathrm{R}}$. In the final state, the opposite limit $\chi_{2\mathrm{R}} \to \infty$ with keeping $\chi_{1\mathrm{R}}$ finite and $\chi_{1\mathrm{R}} \to \infty$ with $|\chi_{2\mathrm{R}}| < \infty$ yields

$$Q \simeq Q_1^{\mathrm{fin}} + Q_2^{\mathrm{fin}}, \tag{116}$$

where

$$Q_j^{\mathrm{fin}} = \sqrt{2}k_{j\mathrm{R}}\mathrm{sech}\left(\chi_{j\mathrm{R}} + \rho_j/2 + r\right)\Pi_j e^{\mathrm{i}(\chi_{j\mathrm{I}}+\sigma_j)}, \tag{117}$$

with

$$r = 2\ln\left|\frac{k_1 - k_2}{k_1 + k_2^*}\right|, \tag{118}$$

$$\sigma_1 = 2\arg\left(\frac{k_1 - k_2}{k_1 + k_2^*}\right),\ \sigma_2 = 2\arg\left(\frac{k_2 - k_1}{k_2 + k_1^*}\right). \tag{119}$$

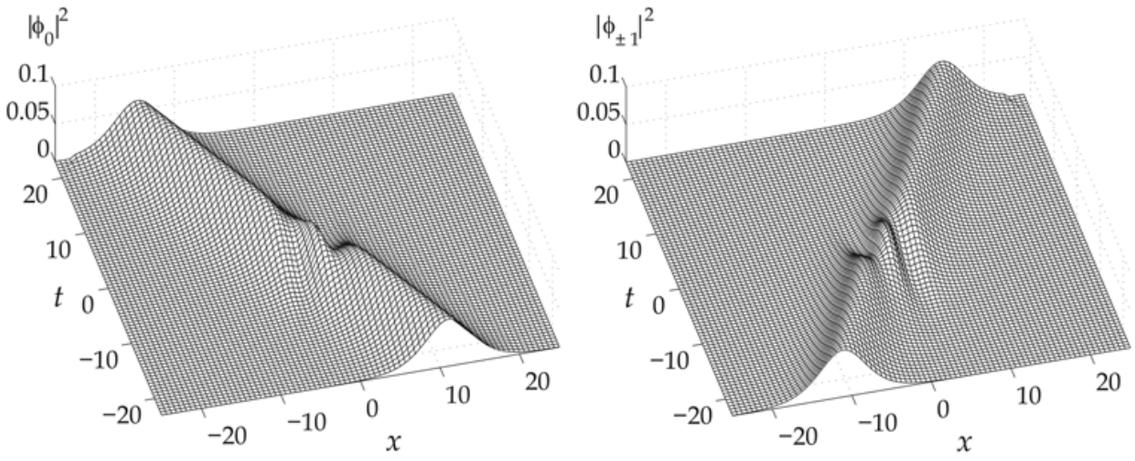

(a) (b)

Fig. 2. Density plots of $|\phi_0|^2$ (a) and $|\phi_{\pm 1}|^2$ (b) for a polar-polar collision. Soliton 1 (left mover) carries only 0 component and soliton 2 (right mover) consists of ±1 components. The parameters used here are $k_1 = 0.25 - 0.25\mathrm{i}$, $k_2 = -0.5 + 0.25\mathrm{i}$, $\alpha_1 = 1/\sqrt{2}$, $\beta_1 = \gamma_1 = 0$, $\alpha_2 = 0$, $\beta_2 = \gamma_2 = 1/\sqrt{2}$.

Equations (115) and (117) are the same form as polar one-soliton solution (105). Collisional effects appear only in the position shift (118) and the phase shifts (119). In Figs. 2, we show the polar-polar collision with $\alpha_1 = 1/\sqrt{2}$, $\beta_1 = \gamma_1 = 0$ and $\alpha_2 = 0$, $\beta_2 = \gamma_2 = 1/\sqrt{2}$. Thus, the partial number N_j, magnetization $\mathbf{F}_j$, momentum P_j, and energy E_j are defined for the asymptotic form of soliton-j and calculated in the same manner as the previous section. The integrals of motion are represented by the sum of those quantities for each soliton. Moreover, we can prove that

$$N_j = 4|k_{j\mathrm{R}}|, \qquad |\mathbf{F}_j| = 0, \qquad P_j = N_j \hbar k_{j\mathrm{I}}, \qquad E_j = N_j c(k_{j\mathrm{I}}^2 - k_{j\mathrm{R}}^2/3), \tag{120}$$

which are by themselves conserved through the collision. In this sense, the polar-polar collision is basically the same as that of the single-component NLS equation.

7.2 Polar-ferromagnetic solitons collision

Under the condition (112), we set soliton 1 to be polar soliton and soliton 2 to be ferromagnetic soliton:

$$|\det \Pi_1| = 1/2, \qquad |\det \Pi_2| = 0. \tag{121}$$

Then, the initial state is represented by eq. (114) with

$$Q_1^{\mathrm{in}} = \sqrt{2} k_{1\mathrm{R}} \mathrm{sech}(\chi_{1\mathrm{R}} + \rho_1/2) \Pi_1 \mathrm{e}^{\mathrm{i}\chi_{1\mathrm{I}}}, \tag{122a}$$

$$Q_2^{\mathrm{in}} = k_{2\mathrm{R}} \mathrm{sech}(\chi_{2\mathrm{R}} + \rho_2/2) \Pi_2 \mathrm{e}^{\mathrm{i}\chi_{2\mathrm{I}}}. \tag{122b}$$

The final state is given by eq. (116) with

$$Q_1^{\text{fin}} = 2k_{1\text{R}} \frac{\tilde{\Pi}_1 \mathrm{e}^{-(\chi_{1\text{R}}+\rho_1/2+\delta)} + \left(\sigma_y \tilde{\Pi}_1^{\dagger} \sigma_y\right) \det\tilde{\Pi}_1 \mathrm{e}^{\chi_{1\text{R}}+\rho_1/2+\delta}}{\mathrm{e}^{-(2\chi_{1\text{R}}+\rho_1+2\delta)} + 1 + \mathrm{e}^{2\chi_{1\text{R}}+\rho_1+2\delta} |\det\tilde{\Pi}_1|^2} \mathrm{e}^{\mathrm{i}\chi_{1\text{I}}}, \tag{123a}$$

$$Q_2^{\text{fin}} = k_{2\text{R}} \operatorname{sech}(\chi_{2\text{R}} + \rho_2/2 + r)\, \Pi_2 \mathrm{e}^{\mathrm{i}(\chi_{2\text{I}}+\sigma_2)}. \tag{123b}$$

Here we have defined

$$\mathrm{e}^{2\delta} = \left|\frac{k_1 - k_2}{k_1 + k_2^*}\right|^2 \left\{1 + \frac{(k_1 + k_1^*)^2 (k_2 + k_2^*)^2}{|k_1 + k_2^*|^2 |k_1 - k_2|^2} \left|\mathrm{tr}\left(\Pi_1 \Pi_2^{\dagger}\right)\right|^2\right\}, \tag{124}$$

$$\tilde{\Pi}_1 = \mathrm{e}^{-\delta}\left\{\Pi_1 - \frac{k_2 + k_2^*}{k_1 + k_2^*}\left(\Pi_1 \Pi_2^{\dagger} \Pi_2 + \Pi_2 \Pi_2^{\dagger} \Pi_1\right) + \left(\frac{k_2 + k_2^*}{k_1 + k_2^*}\right)^2 \mathrm{tr}\left(\Pi_1 \Pi_2^{\dagger}\right) \Pi_2\right\}, \tag{125}$$

and also used eqs. (118), (119). Normalization of the new polarization matrix (125) turns out to be unity,

$$||\tilde{\Pi}_1||_2 = \sqrt{2|\tilde{\alpha}_1|^2 + |\tilde{\beta}_1|^2 + |\tilde{\gamma}_1|^2} = 1. \tag{126}$$

The determinant of it becomes

$$\det\tilde{\Pi}_1 = \mathrm{e}^{-2\delta}\left(\frac{k_1 - k_2}{k_1 + k_2^*}\right)^2 \det\Pi_1. \tag{127}$$

We can see clearly that the initial polar soliton breaks into a split type, $\tilde{A}_1 \equiv (2|\det\tilde{\Pi}_1|)^{-1} > 1$, after the collision with a ferromagnetic one. Only when $\left|\mathrm{tr}\left(\Pi_1 \Pi_2^{\dagger}\right)\right| = 0$, where the spinor part of wave function of two initial solitons is orthogonal to each other, we have $\tilde{A}_1 = 1$. Then, eqs. (123) are reduced to

$$Q_1^{\text{fin}} = \sqrt{2} k_{1\text{R}} \operatorname{sech}(\chi_{1\text{R}} + \rho_1/2 + r)\, \Pi_1 \mathrm{e}^{\mathrm{i}(\chi_{1\text{I}}+\sigma_1)}, \tag{128a}$$

$$Q_2^{\text{fin}} = k_{2\text{R}} \operatorname{sech}(\chi_{2\text{R}} + \rho_2/2 + r)\, \Pi_2 \mathrm{e}^{\mathrm{i}(\chi_{2\text{I}}+\sigma_2)}. \tag{128b}$$

which means that the polar soliton keeps its shape against the collision and shows no mixing among the internal states except for the total phase shift. On the other hand, because of the total spin conservation, the ferromagnetic soliton always retains its polarization matrix and shows only the position and phase shifts similar to those of the polar-polar case.
In Fig. 3, we have density plots of a polar-ferromagnetic collision with the parameters shown in the caption. These pictures correspond to each component of the exact two-soliton solution for one collisional run. For simplicity, we choose the parameters to have $|\phi_1| = |\phi_{-1}|$. The polar soliton (soliton 1) initially prepared in $m_F = \pm 1$ are switched into a soliton with a large population in $m_F = 0$ and the remnant of $m_F = \pm 1$ after the collision. Through the collision, the ferromagnetic soliton (soliton 2) plays only a switcher, showing no mixing in the internal state of itself outside the collisional region, as clearly seen in eq. (123b). In general, this kind of a drastic internal shift of polar soliton is likely observed for large values of $\left|\mathrm{tr}\left(\Pi_1 \Pi_2^{\dagger}\right)\right|$ which appears in eqs. (124), (125). Although all the conserved quantities such as the number of particles and the averaged spin of individual solitons are

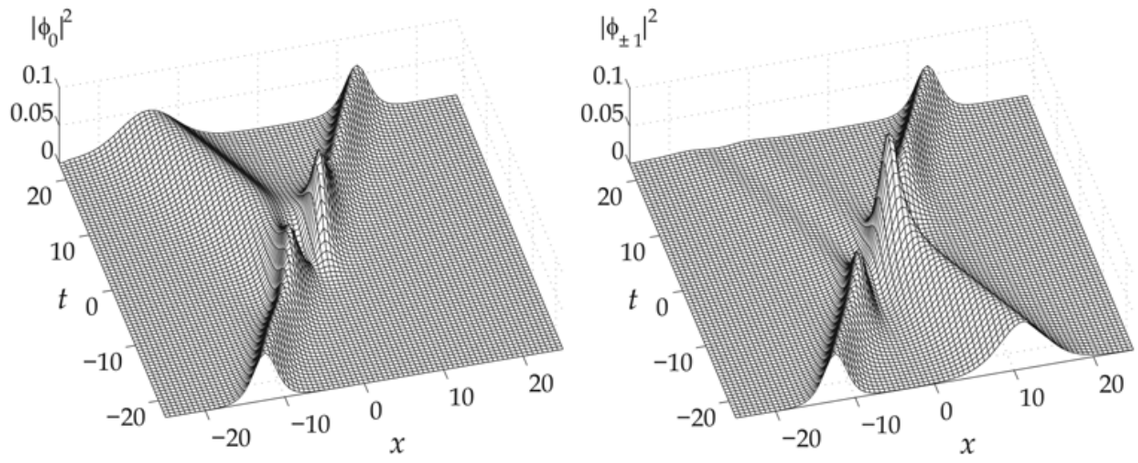

(a) (b)

Fig. 3. Density plots of $|\phi_0|^2$ (a) and $|\phi_{\pm 1}|^2$ (b) for a polar-ferromagnetic collision. Soliton 1 (left mover) is a polar soliton and soliton 2 (right mover) is a ferromagnetic soliton. The parameters used here are $k_1 = 0.25 - 0.25\mathrm{i}$, $k_2 = -0.5 + 0.25\mathrm{i}$, $\alpha_1 = 0$, $\beta_1 = \gamma_1 = 1/\sqrt{2}$, $\alpha_2 = \beta_2 = \gamma_2 = 1/2$.

invariant during this type of collision, the fraction of each component can vary not only in each soliton level but also in the total after the collision. This contrasts to an intensity coupled multicomponent NLS equation in which the total distribution among all components is invariant throughout soliton collisions while a switching phenomenon similar to Fig. 3 can be observed (Radhakrishnan et al.; 1997).

7.3 Ferromagnetic-ferromagnetic solitons collision

Finally, we discuss the collision between two ferromagnetic solitons,

$$\det \Pi_1 = \det \Pi_2 = 0. \tag{129}$$

The asymptotic forms are obtained for the initial state, $Q \simeq Q_1^{\mathrm{in}} + Q_2^{\mathrm{in}}$ where

$$Q_j^{\mathrm{in}} = k_{j\mathrm{R}} \mathrm{sech}(\chi_{j\mathrm{R}} + \rho_j/2)\Pi_j \mathrm{e}^{\mathrm{i}\chi_{j\mathrm{I}}}. \tag{130}$$

and for the final state, $Q \simeq Q_1^{\mathrm{fin}} + Q_2^{\mathrm{fin}}$ where

$$Q_j^{\mathrm{fin}} = k_{j\mathrm{R}} \mathrm{sech}\left(\chi_{j\mathrm{R}} + \rho_j/2 + s\right) \tilde{\Pi}_j \mathrm{e}^{\mathrm{i}\chi_{j\mathrm{I}}}. \tag{131a}$$

Here we have defined

$$s = \ln\left\{1 - \frac{(k_1 + k_1^*)(k_2 + k_2^*)}{|k_1 + k_2^*|^2} \left|\mathrm{tr}\left(\Pi_1 \Pi_2^\dagger\right)\right|\right\}, \tag{132}$$

and, for $(j, l) = (1,2)$ or $(2,1)$,

$$\tilde{\Pi}_j = \mathrm{e}^{-s}\left\{\Pi_j - \frac{k_l + k_l^*}{k_j + k_l^*}\left(\Pi_j \Pi_l^\dagger \Pi_l + \Pi_l \Pi_l^\dagger \Pi_j\right) + \left(\frac{k_l + k_l^*}{k_j + k_l^*}\right)^2 \mathrm{tr}\left(\Pi_j \Pi_l^\dagger\right)\Pi_l\right\}, \tag{133}$$

which are shown to be normalized in unity,

$$||\tilde{\Pi}_j||_2 = \sqrt{2|\tilde{\alpha}_j|^2 + |\tilde{\beta}_j|^2 + |\tilde{\gamma}_j|^2} = 1. \tag{134}$$

Each polarization matrix Π_j of a ferromagnetic soliton can be expressed by three real variables τ_j, θ_j, φ_j as

$$\Pi_j = \mathrm{e}^{\mathrm{i}\tau_j} \begin{pmatrix} \cos^2\frac{\theta_j}{2}\mathrm{e}^{-\mathrm{i}\varphi_j} & \cos\frac{\theta_j}{2}\sin\frac{\theta_j}{2} \\ \cos\frac{\theta_j}{2}\sin\frac{\theta_j}{2} & \sin^2\frac{\theta_j}{2}\mathrm{e}^{\mathrm{i}\varphi_j} \end{pmatrix}. \tag{135}$$

In this expression, the polarization matrices in the initial state Π_j and in the final state $\tilde{\Pi}_j$ are given by

$$\Pi_j = \mathrm{e}^{\mathrm{i}\tau_j}\mathbf{u}_j \cdot \mathbf{u}_j^T, \qquad \tilde{\Pi}_j = \mathrm{e}^{-s+\mathrm{i}\tau_j}\tilde{\mathbf{u}}_j \cdot \tilde{\mathbf{u}}_j^T, \tag{136}$$

where, with $(j, l) = (1,2), (2,1)$,

$$\mathbf{u}_j = \left(\cos\frac{\theta_j}{2}\mathrm{e}^{-\mathrm{i}\frac{\varphi_j}{2}}, \sin\frac{\theta_j}{2}\mathrm{e}^{\mathrm{i}\frac{\varphi_j}{2}}\right)^T, \qquad \tilde{\mathbf{u}}_j = \mathbf{u}_j - \frac{k_l + k_l^*}{k_j + k_l^*}\left(\mathbf{u}_l^\dagger \cdot \mathbf{u}_j\right)\mathbf{u}_l. \tag{137}$$

This defines the collision property for the ferromagnetic-ferromagnetic soliton collision.
We can gain a better understanding of the collision between two ferromagnetic solitons by recasting it in terms of the spin dynamics. The total spin conservation restricts the motion of the spin of each soliton on a circumference around the total spin axis [Fig. 4(a)]. It will be interpreted as a spin precession around the total magnetization.
We calculate the magnetization for each soliton to investigate their collision. In the initial state, following eq. (99), we have the spin of soliton-j as

$$\mathbf{F}_j = 2|k_{j\mathrm{R}}|\left(\sin\theta_j\cos\varphi_j, \sin\theta_j\sin\varphi_j, \cos\theta_j\right)^T. \tag{138}$$

Thanks to the scattering property (137), the final state spins can be obtained through $\mathbf{F}_{1,2}$ by

$$\tilde{\mathbf{F}}_j = \mathrm{e}^{-s}\left[\left\{1 - \frac{2k_{l\mathrm{R}}(k_{1\mathrm{R}} + k_{2\mathrm{R}})}{|k_1 + k_2^*|^2}\right\}\mathbf{F}_j + \frac{k_{2\mathrm{I}} - k_{1\mathrm{I}}}{|k_1 + k_2^*|^2}(\mathbf{F}_j \times \mathbf{F}_l) + \left\{\mathrm{e}^s - 1 + \frac{2k_{j\mathrm{R}}(k_{1\mathrm{R}} + k_{2\mathrm{R}})}{|k_1 + k_2^*|^2}\right\}\mathbf{F}_l\right], \tag{139}$$

where

$$\mathrm{e}^s = 1 + \frac{|\mathbf{F}_\mathrm{T}|^2 - (|\mathbf{F}_1| - |\mathbf{F}_2|)^2}{4|k_1 + k_2^*|^2}. \tag{140}$$

The conserved total spin, $\mathbf{F}_\mathrm{T} \equiv \mathbf{F}_1 + \mathbf{F}_2 = \tilde{\mathbf{F}}_1 + \tilde{\mathbf{F}}_2$, is given by

$$\mathbf{F}_\mathrm{T} = \begin{pmatrix} 2|k_{1\mathrm{R}}|\sin\theta_1\cos\varphi_1 + 2|k_{2\mathrm{R}}|\sin\theta_2\cos\varphi_2 \\ 2|k_{1\mathrm{R}}|\sin\theta_1\sin\varphi_1 + 2|k_{2\mathrm{R}}|\sin\theta_2\sin\varphi_2 \\ 2|k_{1\mathrm{R}}|\cos\theta_1 + 2|k_{2\mathrm{R}}|\cos\theta_2 \end{pmatrix}. \tag{141}$$

Considering spin rotation around the total spin $\mathbf{F}_{\mathrm{T}}$, we can find 'rotated spin' as

$$\mathbf{F}_j^{\mathrm{rot}} = f^{-1}(\varphi)h^{-1}(\theta)f(\omega)h(\theta)f(\varphi)\mathbf{F}_j, \tag{142}$$

where

$$f(\varphi) = \begin{pmatrix} \cos\varphi & \sin\varphi & 0 \\ -\sin\varphi & \cos\varphi & 0 \\ 0 & 0 & 1 \end{pmatrix}, \qquad h(\theta) = \begin{pmatrix} \cos\theta & 0 & -\sin\theta \\ 0 & 1 & 0 \\ \sin\theta & 0 & \cos\theta \end{pmatrix}, \tag{143}$$

with

$$\varphi = \arctan\frac{F_{\mathrm{T}}^y}{F_{\mathrm{T}}^x}, \qquad \theta = \arccos\frac{F_{\mathrm{T}}^z}{|\mathbf{F}_{\mathrm{T}}|}. \tag{144}$$

The rotation angle ω is determined by setting $\mathbf{F}_1^{\mathrm{rot}} = \tilde{\mathbf{F}}_1$ through eqs. (139) and (142),

$$\cos\omega = \frac{4(k_{1\mathrm{I}} - k_{2\mathrm{I}})^2 - |\mathbf{F}_{\mathrm{T}}|^2}{4(k_{1\mathrm{I}} - k_{2\mathrm{I}})^2 + |\mathbf{F}_{\mathrm{T}}|^2}, \qquad \sin\omega = \frac{4(k_{2\mathrm{I}} - k_{1\mathrm{I}})|\mathbf{F}_{\mathrm{T}}|}{4(k_{1\mathrm{I}} - k_{2\mathrm{I}})^2 + |\mathbf{F}_{\mathrm{T}}|^2}. \tag{145}$$

For the case that the magnitudes of the amplitude and velocity for each ferromagnetic soliton are, respectively, identical with each other, $|k_{1\mathrm{R}}| = |k_{2\mathrm{R}}| \equiv N_{\mathrm{T}}/4$, $|k_{1\mathrm{I}}| = |k_{2\mathrm{I}}| \equiv k_{\mathrm{I}}$, the final state magnetizations (139) are given by

$$\tilde{\mathbf{F}}_j = \cos^2\frac{\omega}{2}\mathbf{F}_j + \sin\omega\frac{(\mathbf{F}_j \times \mathbf{F}_l)}{|\mathbf{F}_{\mathrm{T}}|} + \sin^2\frac{\omega}{2}\mathbf{F}_l, \tag{146}$$

where $(j, l) = (1,2), (2,1)$. The rotation angle ω depends only on the ratio $k_{\mathrm{I}}/k_{\mathrm{R}}$ and the magnitude of the normalized total magnetization, $\mathcal{F} \equiv |\mathbf{F}_{\mathrm{T}}|/N_{\mathrm{T}}$, as

$$\omega = 2\arccos\left(\left[1 + \left(\frac{k_{\mathrm{R}}}{k_{\mathrm{I}}}\right)^2 \mathcal{F}^2\right]^{-1/2}\right). \tag{147}$$

The principal value should be taken for the arccosine function: $0 \le \arccos x \le \pi$.
Setting $k_{\mathrm{I}} \gg k_{\mathrm{R}}$ in eq. (147), one gets the small rotation angle, $\omega \simeq 0$. In the opposite case, $k_{\mathrm{I}} \ll k_{\mathrm{R}}$, each spin of two colliding solitons almost reverses its orientation, $\omega \simeq \pi$. Recall that k_{I} is the speed of soliton. We can understand these phenomena since a slower soliton spends the longer time inside the collisional region. Figure 4 shows the velocity dependence of the rotation angle for various initial normalized spins. When $\mathcal{F} = 1$, which corresponds to the case of antiparallel spin collision, the spin precession can not occur as shown by the dotted line in Fig. 4(b).
In Fig. 5–Fig. 7, we give examples of this type of collisions for different k_{I}, with the other conditions fixed, to illustrate the velocity dependence. The initial normalized spin for the parameter set given in the captions is $\mathcal{F} = 0.5$. The rotation angles are $\omega \simeq 0.2\pi$, 0.5π and 0.9π for Fig. 5, Fig. 6 and Fig. 7, respectively. The internal shift $\phi_1 \to \phi_{-1}$, and vice versa, gradually increase by slowing down the velocity of the solitons.

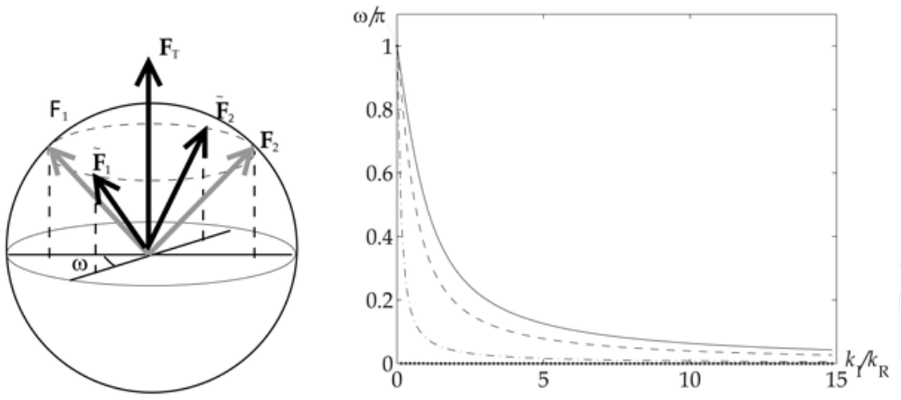

(a) (b)

Fig. 4. (a) Schematic of spin precession of two colliding ferromagnetic solitons. (b) Velocity dependence of the rotational angle in spin precession for the different initial relative angles, $\mathcal{F} = 1$ (solid line), 0.5 (dashed line), 0.0157π (dash-dot line) and 0 (dotted line).

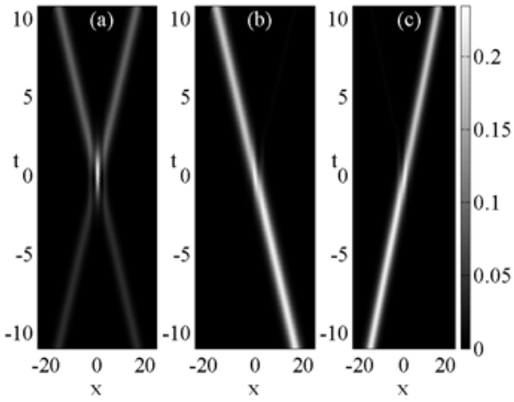

Fig. 5. Density plots of (a) $|\phi_0|^2$, (b) $|\phi_1|^2$ and (c) $|\phi_{-1}|^2$ for a fast ferromagnetic-ferromagnetic collision. The parameters used here are $k_1 = 0.5 - 0.75i$, $k_2 = -0.5 + 0.75i$, $\alpha_1 = 4/17$, $\beta_1 = 16/17$, $\gamma_1 = 1/17$, $\alpha_2 = 4/17$, $\beta_2 = 1/17$, $\gamma_2 = 16/17$.

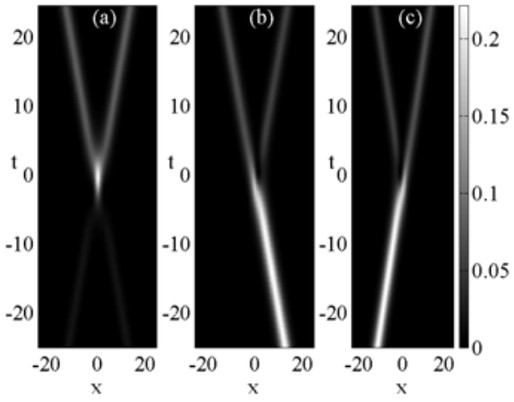

Fig. 6. Density plots of (a) $|\phi_0|^2$, (b) $|\phi_1|^2$ and (c) $|\phi_{-1}|^2$ for a medium speed ferromagnetic-ferromagnetic collision. The parameters are the same as those of Fig. 5 except for $k_{1I} = -0.25$, $k_{2I} = 0.25$.

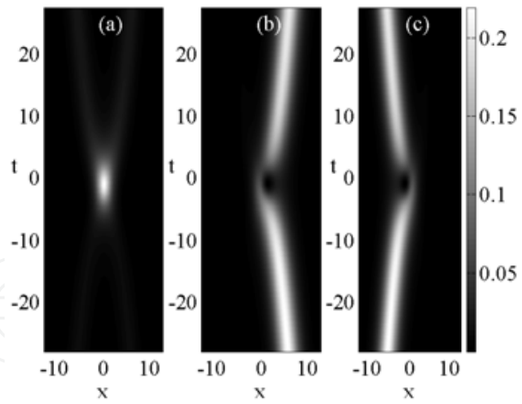

Fig. 7. Density plots of (a) $|\phi_0|^2$, (b) $|\phi_1|^2$ and (c) $|\phi_{-1}|^2$ for a slow ferromagnetic-ferromagnetic collision. The parameters are the same as those of Fig. 5 except for $k_{1I} = -0.05$, $k_{2I} = 0.05$.

8. Concluding remarks

The soliton properties in spinor Bose–Einstein condensates have been investigated. Considering two experimental achievements in atomic condensates, the matter-wave soliton and the spinor condensate, at the same time, we have predicted some new phenomena.

Based on the results provided in Sec. 2–4, in Sec. 5 we have introduced the new integrable model which describes the dynamics of the multicomponent matter-wave soliton. The key idea is finding the integrable condition of the original coupled nonlinear equations, i.e., the spinor GP equations derived in Sec. 4. The integrable condition expressed by the coupling constants, which is accessible via the confinement induced resonance explained in Sec. 3.

In Sec. 6, we classify the one-soliton solution. There exist two distinct spin states: ferromagnetic, $|\mathbf{F}_T| = N_T$ and polar, $|\mathbf{F}_T| = 0$. In the ferromagnetic state, the spatial part and the spinor part of the soliton are factorized (ferromagnetic soliton). In the polar state, dissimilar shaped solitons which we call polar soliton for $\mathbf{f}(x) = 0$ and split soliton otherwise are energetically degenerate. The polar soliton has one peak and the space-spinor factorization holds. On the other hand, a split soliton consists of twin peaks and the three components show different profiles. Changing the polarization parameters one may control the peak distance continuously.

In Sec. 7, we have analyzed two-soliton solutions which rule collisional phenomena of the multiple solitons. Specifying the initial conditions, we have demonstrated two-soliton collisions in three characteristic cases: polar-polar, polar-ferromagnetic, ferromagnetic-ferromagnetic. In their collisions, the polar soliton is always "passive" which means that it does not rotate its partner's polarization while the ferromagnetic soliton does. Thus, in the polar-ferromagnetic collision, one can use the polar soliton as a signal and ferromagnetic soliton as a switch to realize a coherent matter-wave switching device. Collision of two ferromagnetic solitons can be interpreted as the spin precession around the total spin. The rotation angle depends on the total spin, amplitude and velocity of the solitons. Only varying the velocity induces drastic change of the population shifts among the components.

Stability of spinor solitons has been investigated numerically and perturbatively (Li et al.; 2005) (Dabrowska-Wüster et al.; 2007) (Doktorov et al.; 2008). It is also interesting to pursue

the soliton dynamics of spinor condensates under longitudinal harmonic trap (Zhang et al.; 2007). Recently, the integrability of the spinor GP equation has been studied in detail (Gerdjikov et al.; 2009). The behavior of spinor solitons shows a variety of nonlinear dynamics and it is worth exploring them experimentally.

9. Acknowledgment

This work was supported by Grant-in-Aid for Scientific Research No. 20740182 from MEXT.

10. References

Dabrowska-Wüster, B. J.; Ostrovskaya, E. A.; Alexander, T. J.; Kivshar, Y. S. (2007). Multicomponent gap solitons in spinor Bose–Einstein condensates. *Physical Review A*, 75, 2, (April 2008) 023617-1–023617-11, ISSN 1094-1622.

Doktorov, E. V.; Wang, J. D.; Yang, J. K. (2008). Perturbation theory for bright spinor Bose-Einstein condensate solitons. *Physical Review A*, 77, 4, (April 2008) 043617-1–043617-11, ISSN 1094-1622.

Gerdjikov, V.S.; Kostov, N.A.; Valchev, T. I. (2009). Solutions of multi-component NLS models and Spinor Bose–Einstein condensates. *Physica D: Nonlinear Phenomena*, 238, 15, (July 2009) 1306–1310, ISSN 0167-2789.

Ieda, J.; Tsurumi, T.; Wadati, M. (2001). Bose–Einstein Condensation of Ideal Bose Gases. *Journal of the Physical Society of Japan*, 70, 5, (May 2001) 1256–1259, ISSN 1347-4073.

Ieda, J.; Miyakawa, T.; Wadati, M. (2004). Exact Analysis of Soliton Dynamics in Spinor Bose–Einstein Condensates. *Physical Review Letters*, 93, 19, (November 2004) 194102-1–194102-4, ISSN 1079-7114.

Ieda, J.; Miyakawa, T.; Wadati, M. (2004). Matter-Wave Solitons in an F=1 Spinor Bose–Einstein Condensate. *Journal of the Physical Society of Japan*, 73, 11, (November 2004) 2996–3007, ISSN 1347-4073.

Ieda, J.; Uchiyama, M.; Wadati, M. (2007). Inverse scattering method for square matrix nonlinear Schrodinger equation under nonvanishing boundary conditions. *Journal of Mathematical Physics*, 48, 1, (January 2007) 013507-1–013507-19, ISSN 1089-7658.

Khaykovich, L.; Schreck, F.; Ferrari, G.; Bourdel, T.; Cubizolles, J.; Carr, L. D.; Castin, Y.; Salomon, C. (2002). Formation of a Matter-Wave Bright Soliton. *Science*, 96, 5571, (May 2002) 1290–1293, ISSN 1095-9203.

Kanamoto, R; Saito, H; Ueda, M. (2003). Quantum phase transition in one-dimensional Bose– Einstein condensates with attractive interactions. *Physical Review A*, 67, 1, (January 2003) 013608-1–013608-7, ISSN 1094-1622.

Li, L.; Li, Z.; Malomed, B. A.; Mihalache, D.; Liu, W. M. (2005). Exact soliton solutions and nonlinear modulation instability in spinor Bose–Einstein condensates. *Physical Review A*, 72, 3, (September 2005) 033611-1–033611-11, ISSN 1094-1622.

Meystre, P. (2001). *Atom Optics*, Springer-Verlag New York, Inc., New York.

Olshanii, M. (1998). Atomic Scattering in the Presence of an External Confinement and a Gas of Impenetrable Bosons. *Physical Review Letters*, 81, 5, (August 1998) 938–941, ISSN 1079-7114.

Pethick, C. J. & Smith, H. (2002). *Bose–Einstein condensation in dilute Gases*, Cambridge University Press, Cambridge. Also 2nd ed. (2008).

Stenger, J.; Inoue, S.; Stamper-Kurn, D. M.; Miesner, M. R.; Chikkatur, A. P.; Ketterle, W. (1998). Spin domains in ground-state Bose–Einstein condenstate. *Nature*, 396, 6709, (November 1998) 345–348, ISSN 0028-0836.

Radhakrishnan, R.; Lakshmanan, M.; Hietarinta, J. (1997). Inelastic collision and switching of coupled bright solitons in optical fibers. *Physical Review E*, 56, 2, (August 1997) 2213–2216, ISSN 1550-2376.

Strecker, K. E.; Partridge, G. B.; Truscott, A. G.; Hulet, R. G. (2002). Formation and propagation of matter-wave soliton trains. *Nature*, 417, (May 2002) 150–153, ISSN 0028-0836.

Tsuchida, T. & Wadati, M. (1998). The Coupled Modified Korteweg–de Vries Equations. *Journal of the Physical Society of Japan*, 67, 4, (April 1998) 1175–1187, ISSN 1347-4073.

Uchiyama, M.; Ieda, J.; Wadati, M. (2006). Dark Solitons in F=1 Spinor Bose–Einstein Condensate. *Journal of the Physical Society of Japan*, 75, 6, (June 2006), 064002-1–064002-9, ISSN 1347-4073.

Uchiyama, M.; Ieda, J.; Wadati, M. (2007). Multicomponent Bright Solitons in F=2 Spinor Bose– Einstein Condensates. *Journal of the Physical Society of Japan*, 76, 7, (July 2007), 074005- 1–074005-6, ISSN 1347-4073.

Ueda, M. & Koashi, M. (2002). Theory of spin-2 Bose–Einstein condensates: Spin correlations, magnetic response, and excitation spectra. *Physical Review A*, 65, 6, (May 2002), 063602-1–063602-22, ISSN 1094-1622.

Zhang, W.; Müstecaplıoğlu, Ö. E.; You, L. (2007). Solitons in a trapped spin-1 atomic condensate. *Physical Review A*, 75, 4, (April 2007), 043601-1–043601-8, ISSN 1094-1622.

Nonlinear Dynamics

Edited by Todd Evans

ISBN 978-953-7619-61-9
Hard cover, 366 pages
Publisher InTech
Published online 01, January, 2010
Published in print edition January, 2010

This volume covers a diverse collection of topics dealing with some of the fundamental concepts and applications embodied in the study of nonlinear dynamics. Each of the 15 chapters contained in this compendium generally fit into one of five topical areas: physics applications, nonlinear oscillators, electrical and mechanical systems, biological and behavioral applications or random processes. The authors of these chapters have contributed a stimulating cross section of new results, which provide a fertile spectrum of ideas that will inspire both seasoned researches and students.

INTECH
open science | open minds

InTech Europe
University Campus STeP Ri
Slavka Krautzeka 83/A
51000 Rijeka, Croatia
Phone: +385 (51) 770 447
Fax: +385 (51) 686 166
www.intechopen.com

InTech China
Unit 405, Office Block, Hotel Equatorial Shanghai
No.65, Yan An Road (West), Shanghai, 200040, China
中国上海市延安西路65号上海国际贵都大饭店办公楼405单元
Phone: +86-21-62489820
Fax: +86-21-62489821

IntechOpen